OPTICS OF BEAM RECIRCULATION IN THE CEBAF CW LINAC

David R. Douglas
Continuous Electron Beam Accelerator Facility
12070 Jefferson Avenue
Newport News, VA. 23606

Abstract

The use of recirculation in linear accelerator designs requires beam transport systems that will not degrade beam quality. We present a design for the transport lines to be used during recirculation in the CEBAF accelerator. These beam lines are designed to avoid beam degradation through synchrotron radiation excitation or betatron motion mismatch, are insensitive to errors commonly encountered during beam transport, and are optimized for electron beams with energies of 0.5 to 6.0 GeV. Optically, they are linearly isochronous second order achromats based on a "missing magnet" FODO structure. We give lattice specifications for, and results of analytic estimates and numerical simulations of the performance of, the beam transport system.

Accelerator Overview

The CEBAF accelerator is a recirculating cw linac designed to generate electron beams of energy 0.5 to 4.0 GeV at a 1 GeV emittance of $\epsilon = 2. \times 10^{-9}$ m-rad with a momentum spread $4 \times (\sigma_E/E) = 1. \times 10^{-4}$. The machine (described elsewhere[1], shown in Figure 1) consists of a 50 MeV injector, two superconducting cw "linac segments", and a recirculator. The linac segments simultanieously accelerate four beams at different energies; the energy gain is 0.5 GeV per segment. Each beam can be recirculated to make up to four passes through each segment for a final energy of 4.0 GeV. The recirculator consists of two arcs that transport beams from one linac segment to the other for further acceleration. In each arc, a "spreader" separates the beams according to energy. A set of beam lines (one line for each energy) transports the beams to the next linac segment, where they are made collinear using a "recombiner" and injected into the segment.

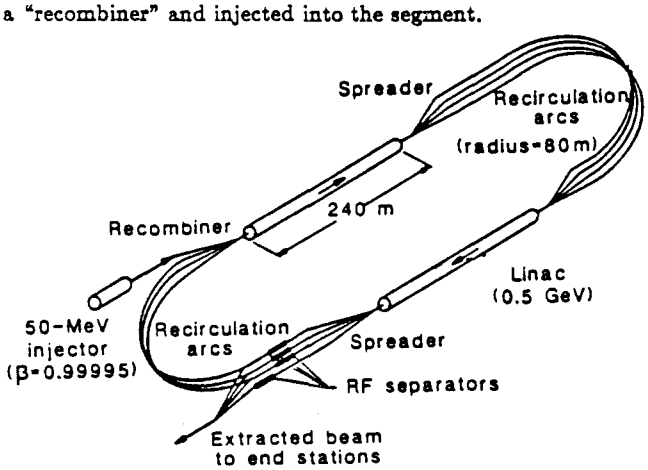

Figure 1. Schematic of CEBAF Recirculating Linac

Here, we focus on the recirculation arc beam lines. The two arcs comprise a total of seven beam lines. For a final energy of 4.0 GeV, the four beam lines at the east end of the machine transport beams at 0.5, 1.5, 2.5 and 3.5 GeV, while the three at the west end carry 1.0, 2.0 and 3.0 GeV beams. Recirculation through these lines introduces two sources of beam quality degradation. The first is "optical" errors. Such errors include mismatches of the beam phase space, distortions generated by optical aberrations in the beam lines, and perturbations due to imperfections in the magnetic fields that bend and focus the beam. The second source of degradation is synchrotron radiation excitation. Radiative excitation increases both the emittance and momentum spread of the electron beam. The lines described here have been designed to insure that such radiation-induced contributions are negligible.

Recirculator Arc Beam Line Requirements

The recirculator arc beam lines were designed to avoid degrading beam quality, rely on mechanically simple magnetic components, and be compatible with a tunnel that could accommodate potential upgrades of linac energy within the existing recirculator housing.

Transport Line Optical Constraints

The requirement of minimal beam degradation can be met by imposing two types of lattice contraints. The first is that the recirculator arc beam line lattices be achromatic, isochronous, and imaging, and will provide a total beam path length that is a multiple of the RF wavelength. These features will facilitate reinjection of the beam into the linac and insure that no betatron or longitudinal mismatch (with resulting phase space dilution) will arise. Achromaticity and isochronicity are achieved by proper transport and matching of the dispersion function; imaging is achieved by choosing optics that lead to an integer number of betatron oscillations in each beam line.

Synchrotron Radiation Effects

The second constraint imposed to avoid beam degradation is that the arcs generate minimal excitation through synchrotron radiation. The radiation-induced energy spread σ_E and emittance blowup $\Delta\epsilon$ occuring when a beam bends though 180° are given by the following expressions (in MKSA units):[2]

$$\sigma_E^2 = 1.182 \times 10^{-33}\mathrm{GeV}^2\ \mathrm{m}^2 \frac{\gamma^7}{\rho^2}$$
$$\Delta\epsilon = 1.32\pi \times 10^{-27}\mathrm{m}^2\ \mathrm{rad} \frac{\gamma^5}{\rho^2}\langle\mathcal{H}\rangle \qquad (1)$$

Here

$$\langle\mathcal{H}\rangle \simeq \left(\frac{1}{L}\right)\int_{bends} ds \left\{\left(\frac{1}{\beta}\right)\left[\eta^2 + \left(\beta\eta' - \frac{1}{2}\beta'\eta\right)^2\right]\right\}$$

with L = orbit length in bending magnets and ρ =orbit radius in bending magnets. The induced energy spread is a function of the bending radius only, but the emittance blowup may be controlled, in part, by the choice of lattice functions.

Beam Line Parameters, Configuration, and Optics

The strong γ dependence of σ_E/E and $\Delta\epsilon$ suggests that only the highest energy beam lines contribute significantly to these blowups. Parametric studies based on (1) confirm this,

and also indicate that the final values of σ_E/E and $\Delta\epsilon$ depend only weakly on the choice of bending radius for the first five beam lines. The bending radii in these beam lines may therefore be reduced without degradation of beam quality. As $\Delta\epsilon$ may be controlled through $\langle\mathcal{H}\rangle$, the bend radius in the final beam line may be set by σ_E/E alone.

The choice of bending radius for the high energy beam lines is driven both by radiation excitation considerations and a desire to accommodate linac energy upgrades within the tunnel defined by the recirculator arcs. Since an upgrade to 6 GeV shortly after machine commissioning will be practical if SRF cavity technology continues to develop as expected[3], we set the bend radius by specifing that $4 \times (\sigma_E/E)$ be on the order of 1×10^{-4} at 6 GeV. Use of (1) indicates that a final bending radius of 30 m satisfies this radiation excitation requirement. In addition, the bend packing fraction in an achromatic, isochronous lattice of the type required here is only 50% or less. Hence, a tunnel of mean radius 60 to 80 m will be required. However, lattices capable of recirculation at even higher energies in a tunnel of 80 m mean radius have been generated[4], so the choice of 30 m final bending radius is also consistent with accommodating energy upgrades within the accelerator housing (using different types of lattices).

Bending radii for lower energy beam lines are constrained by a desire for operational simplicity; this implies that all beam lines be designed in a similar fashion. This has been done by designing the beam lines in a modular fashion; low-energy beam lines are generated from high-energy lines by replacing bending magnets with drift spaces, resetting beam-line focusing magnets to retain the desired optical properties, and adjusting drift lengths to yield a total beam path length equal to a multiple of the RF wavelength. The bending radii for the lower energy beam lines are thus a fraction of the radius for the final 3.5 GeV line, with the fraction being the ratio of the number of bending magnets in the lines. The following numerology for all bending radii has been adopted. A bending radius of approximately 30 m is obtained using 90 m of bending in a beam line. This is provided by 40 dipoles of 2.25 m magnetic length in the 3.0 and 3.5 GeV lines. We use 32 similar dipoles in the 2.5 GeV line, and 16 such dipoles in the four lowest-energy lines.

As noted, the transverse emittance blowup may be controlled by the choice of lattice functions. We have sought to reduce $\langle\mathcal{H}\rangle$ as much as possible consistent with other contraints. This was achieved, together with achromaticity, isochronicity, and imaging, through the use of a four-period structure in each beam line. Each period consists of a modified four-cell FODO structure with "missing magnets." The regular alternation of dipoles and quadrupoles is interrupted; dipoles are replaced by drift spaces to drive the dispersion across the design orbit and create an isochronous structure. The use of four periods per line reduces the maximum and the mean values of the dispersion and betatron functions (thereby reducing $\langle\mathcal{H}\rangle$). The similarity of all beam lines insures that corresponding beam line elements lie in approximately the same location at a given path length; this simplifies tunnel geometry.

Imaging is obtained by tuning each period to 5/4 betatron wavelength. This produces a unit transfer matrix over the four-period arc and yields well-behaved lattice functions. It also allows simple elimination of all linear chromatic aberrations through the use of sextupoles; the resulting beam lines are second-order achromats[5]; all second order transverse aberrations are eliminated. All periods of all lines have been matched to the same betatron function values. This allows each beam line to be treated as identical to all others insofar as matching to the linacs is concerned. The structure of, and the lattice functions for, one period of each type of beam line are illustrated in Figure 2. Table 1 gives lattice specifications, as computed by DIMAD[6], for each beam line.

Figure 2. Structure and Lattice Functions of One Period of Arc Beam Lines

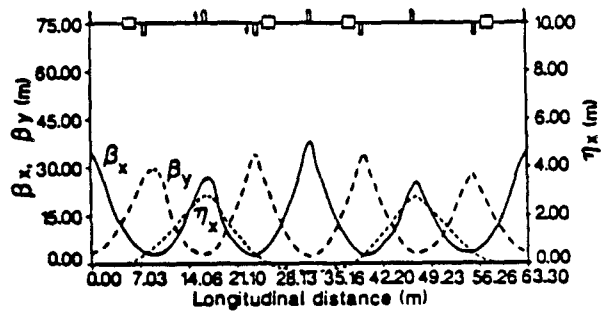

Figure 2a. 0.5-2.0 GeV Beam Lines

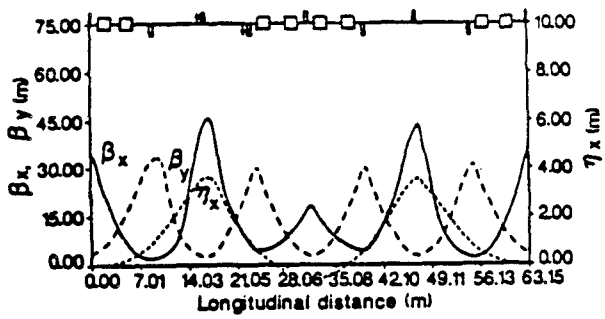

Figure 2b. 2.5 GeV Beam Line

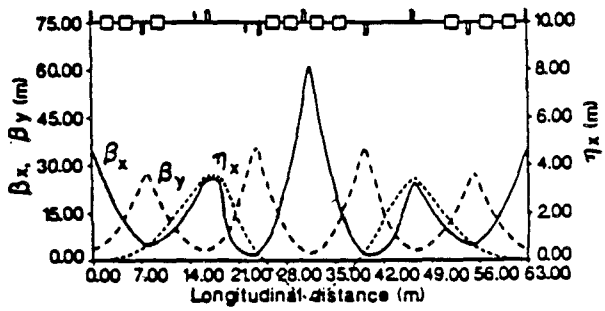

Figure 2c. 3.0-3.5 GeV Beam Lines

Table 1: Beam Line Lattice Properties

Lattice Property	0.5-2.0 GeV Lines	2.5 GeV Line	3.0-3.5 GeV Lines
# Dipoles	16	32	40
Orbit Radius in Dipoles (m)	11.46	22.92	28.65
Dipole Magnetic Length (m)	2.25	2.25	2.25
# Quadrupoles	32	32	32
Min. Quad Focal Length (m)	4.56	4.30	4.36
Phase Advances $\psi_{x,y}$	$2\pi \times 5$	$2\pi \times 5$	$2\pi \times 5$
Matched β_x, β_y (m)	35.,3.5	35.,3.5	35.,3.5
$\langle\mathcal{H}\rangle$ (m)	.114	.167	.269
x,y Natural Chromaticities	-7.6,-8.11	-8.66,-7.76	-9.28,-7.92
# Sexupoles	8	8	8
Peak Sextupole $(B''l/B\rho)$ (m^2)	1.51	1.14	1.24

Beam Line Performance

Effects of Radiative Excitation

Analytic Estimates of synchrotron radiation induced emittance and momentum spread growth are displayed in Figure 3. The results are based on (1), illustrate the cumulative increases for all recirculations, and include the effect of adiabatic damping. The results are well below the design values of the machine, with $\Delta\epsilon = 3.4 \times 10^{-11}$ m-rad compared to $\epsilon = 5 \times 10^{-10}$ m-rad at 4 GeV and $(\sigma_E/E)_{induced} = 1.2 \times 10^{-5}$ compared to $\sigma_E/E = 2.5 \times 10^{-5}$ at 4 GeV.

Figure 3. Radiation Induced Blowups at Start and End of Each Beam Line

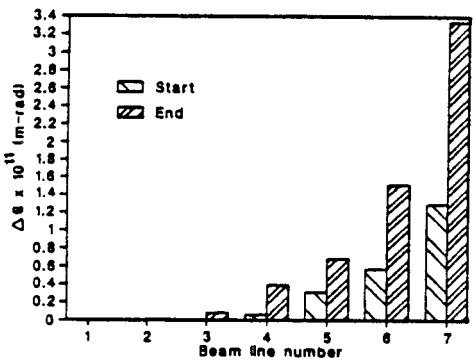

Figure 3a. Induced Emittance Growth

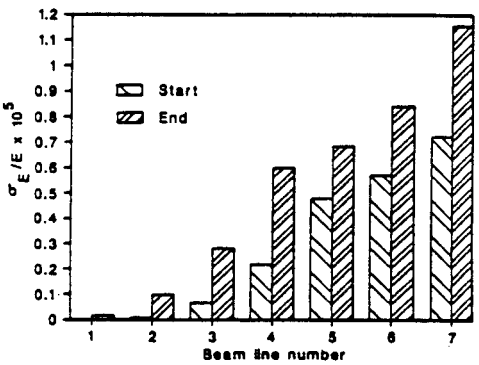

Figure 3b. Induced Momentum Spread

Numerical Simulations have been used to verify analytical estimates. Two independent numerical simulations have been performed. The first used the synchrotron radiation simulation feature of DIMAD to model the motion of 10000 particles through the beam lines. This simulation assumed an approximate gaussian distribution for the radiated photon energy and number spectra, and thus was most appropiate to modeling motion in the high energy beam lines. The second, described elsewhere[7], employed statistics that were correct in the details of the distributions describing the radiation, and hence was appropriate for modeling motion all beam lines. Results from both simulations were consistant and in agreement with analytic estimates.

Effects of Magneto-Optical Perturbations

Analytic Estimates The effect of two types of lattice perturbations has been studied. The first type is errors causing deviations of the design orbit from its nominal path through the centers of all magnetic elements, such as quadrupole misalignments and dipole powering errors. We have determined that rms quadrupole misalignments of 0.2 mm will produce design orbit errors of less than 1 cm in either plane. Random dipole powering errors with rms values of 0.01% will produce design orbit errors of 1.5 mm at the end of the lowest energy beam line (the most sensitive beam line, because it has only 16 dipoles). Systematic dipole errors cancel completely over the line length (because the beam line is an achromat). For this reason, the dipoles in a given beam line will be on a common circuit; any powering errors will then be systematic.

The second type of errors investigated are those producing effects upon motion about the design orbit, such as quadrupole powering errors and error sextupoles. We find that rms quad power supply errors of 0.1% will produce rms betatron function mismatches of 0.4% in β and 0.004 in α, as well as r.m.s. tune variations on the order of 0.002. These are small; the corresponding mismatch-induced emittance increase is less than 6% of the final emittance at 4 GeV. Sextupole errors give smaller effects. If the systematic sextupole component of the bend produces a $\Delta B/B$ of 10^{-4} at 4 cm, then the effective contributed chromaticity will be approximately 10% of the natural chromaticity of the beam line. This is readily compensated with the standard chromaticity correction sextupoles. As the rms random sextupole component should be an order of magnitude smaller, we anticipate no significant effects from the random sextupole.

Numerical Simulations DIMAD has been used to study these perturbation effects. The analytic analysis of the effects of quadrupole misalignments and dipole powering errors was confirmed numerically. In addition, DIMAD indicates that the misaligned orbit can be corrected to better than 0.5 mm rms deviation and 1.5 mm peak deviation using a simple orbit correction scheme consisting of a position monitor (reading horizontal and vertical displacements) and a single correction dipole (acting in the focusing plane) at each quadrupole.

The second order perturbations were also modeled. Simulation with DIMAD indicates that only 10% additional sextupole strength is required to compensate the systematic sextupole in the dipole, and, moreover, that this systematic error has no significant impact on the nonlinear optics. No significant geometric or chromatic aberrations are generated. Finally, using DIMAD we have confirmed that a random sextupole component giving a $\Delta B/B$ of 10^{-5} at 4 cm will not affect the performance of the beam line optics.

Acknowledgements

I would like to thank Christoph Leemann, Richard York, and Joseph Bisognano for useful discussions, and Steve Corneliussen, Geoffrey Krafft, and Peter Kloeppel for editorial assistance. This work was supported by D.O.E. contract # DE-ACO-84ER4015.

References

1. Ch. W. Leemann, these proceedings; CEBAF Conceptual Design Report, CEBAF-PR-86-002, Feb. 1986.
2. M. Sands, SLAC-121 (Nov. 1970)
3. See, *e.g.*, references in 1.
4. D. R. Douglas, unpublished
5. K. L. Brown, I.E.E.E. Trans. Nuc. Sci. NS-26, 3, (1979)
6. R. Servranckx *et. al.* "Users Guide to the program DIMAD", SLAC Report 285 UC-28 (A), May 1985
7. B. Norum, CEBAF-TN0019, 5 Nov. 1985